Journal of Bioscience and Bioengineering
VOL. 127 No. 2, 231–240, 2019

www.elsevier.com/locate/jbiosc

Exopolysaccharides from the fungal endophytic *Fusarium* sp. A14 isolated from *Fritillaria unibracteata* Hsiao et KC Hsia and their antioxidant and antiproliferation effects

Feng Pan, Kai Hou, Dan-Dan Li, Tian-Jiao Su, and Wei Wu*

Department of Production of Special Utilizated Plant, Agronomy College, Sichuan Agricultural University, No. 211, Huimin Rd, Wenjiang Region, Chengdu, 611130 Sichuan, PR China

Received 28 January 2018; accepted 26 July 2018
Available online 1 September 2018

Exopolysaccharides (EPSs) are high-molecular-weight carbohydrates with a wide range of biophysiological activities, such as antioxidant activity, immunostimulatory activity, antitumor activity, hepatoprotective activity, and antifatigue effects. In the present work, two water-soluble EPSs, namely, A14EPS-1 and A14EPS-2, were isolated and purified from the fungal endophytic strain A14 using ethanol precipitation, DEAE-cellulose ion exchange chromatography and Sepharose G-150 gel filtration chromatography. A14EPS-1 (~2.4 × 10^4 Da, the major fraction) was mainly composed of mannose, rhamnose, glucose, galactose, xylose and arabinose with a molar ratio of 0.31:0.55:10.00:0.34:0.03:0.06. The major monosaccharide of A14EPS-1 was pyranose, which was connected by α-glycosidic linkages. And the side chains of A14EPS-1 may be composed of rhamnose, arabinose, glucose and galactose; moreover, the backbone of A14EPS-1 may be composed of rhamnose, xylose, arabinose and glucose. A14EPS-2 (~0.5 × 10^4 Da) was mainly composed of mannose, rhamnose, glucose, galactose, xylose and arabinose in a ratio of 0.16:0.88:10.00:0.39:0.06:0.06. Pyranose was observed in both the α- and β-configurations in A14EPS-2, and the α configuration was dominant. In addition, the results of the bioactivity assays indicated that both A14EPS-1 and A14EPS-2 had moderate antioxidant activity *in vitro*, and A14EPS-2 showed a moderate antiproliferation effect on human hepatocellular carcinoma HepG2 cells.

[**Key words:** *Fritillaria unibracteata* Hsiao et KC Hsia; Fungal endophytic *Fusarium* sp. A14; Exopolysaccharide; Antioxidant activity; Antiproliferation activity]

Polysaccharides, biological macromolecules, are long-chain polymers of monosaccharide units linked by glycosidic bonds. An increasing number of studies have suggested that polysaccharides have a variety of biological activities, such as antioxidant, antitumor, immunoregulatory and anti-inflammatory activities without toxicity (1–3). Microbial exopolysaccharide (EPS) is a kind of polysaccharide produced by microorganisms including bacteria and fungi, and it has good potential economic value (4,5). According to market assessments, bacterial EPSs alone have an annual processing output value of more than $1.25 billion (5). Natural polysaccharides from edible fungi are also widely used in the food, health care, pharmaceutical and other fields (6) and have a larger market. In return, such markets will provide opportunities for the development of microbial EPSs. Correspondingly, in the last decade, interest in EPS has significantly increased (7–9).

Fungal endophytes, which invade or live inside of the tissues of plants without causing any harm to the host (10), are estimated to include one million species (i.e., approximately 1 in 14 of all species of life) (11), including many novel microbes. During a long period of co-evolution, fungal endophytes play multiple physiological and ecological roles for their host plants (12). Positive symbiosis can exist between the fungal endophytes and their hosts, and in such systems, the fungi obtain energy, nutrients and shelter, and in return, they facilitate the growth of their host plants directly or indirectly and improve the resistance of their hosts to abiotic or biotic stresses (13,14). In addition, those fungi living in host plants can secrete different EPSs, which may have an essential role for either the fungi or their hosts, such as the auxiliary scavenging effect to free radicals, under limited growth space and under specific natural environments and in particular lifestyles (9,15). EPS from fungal endophytes, such as As1-1 obtained from endophytic fungus *Aspergillus* sp. Y16, PS-1 obtained from *Fusarium solani* SD5 or the EPS obtained from *Bionectria ochroleuca* M21, possessed various biological activities, such as, *in vitro* antioxidant or antitumor activities (1,16,17). In addition, a large number of compounds are produced by endophytic fungi and show strong bioactivities (18,19). However, the polysaccharides (PSs) originated from endophytic fungi have been the subject of few investigations, and reports on PSs account for less than 1% of studies related to endophytic fungi.

In the present report, two homogeneous EPSs were isolated from the culture medium of a fungal endophytic *Fusarium* sp. A14 derived from *Fritillaria unibracteata* Hsiao et KC Hsia, which is the most commonly used herb with antitussive and expectorant effects in traditional Chinese medicine. In addition, the monosaccharide composition, relative molecular mass (M_r) and partial structure

* Corresponding author. Tel./fax: +86 028 86290870.
E-mail address: ewuwei@sicau.edu.cn (W. Wu).

1389-1723/$ – see front matter
https://doi.org/10.1016/j.jbiosc.2018.07.023

were further analyzed. Then, the *in vitro* antioxidant and anti-proliferation activities of the EPSs were evaluated.

MATERIALS AND METHODS

Microorganism The fungal endophytic *Fusarium* sp. strain A14 (GenBank accession number JF273500) was isolated from healthy bulbs of *F. unibracteata* Hsiao et KC Hsia. The organism was maintained and stored on potato dextrose agar slants at 4°C.

Reagents DEAE-Cellulose (type DE52) was purchased from Whatman (Brantford, UK). Macroporous S-8 and D101 resin were provided by Guangzhou Xiang Bo Biological Technology Co., Ltd. (Guangzhou, China). T-series dextrans of different molecular weights (T-5, T-10, T-40, T-70 and T-500), the standard monosaccharides (D-(+)-mannose, L-rhamnose, D-(+)-galacturonic acid, D-(+)-glucose, D-(+)-galactose, D-(+)-xylose, L-(+)-arabinose, L-(−)-fucose), 1,1-diphenyl-2-picrylhydrazyl (DPPH), and 2,2′-azino-bis (3-ethylbenzthiazoline-6-sulphonic acid) (ABTS) were from Sigma–Aldrich (Shanghai, China). HPLC-grade acetonitrile was purchased from Fisher Scientific Worldwide (Shanghai) Co., Ltd. (Shanghai, China). D_2O (99.9 atom % D) was purchased from Shanghai Macklin Biochemical Co., Ltd. (Shanghai, China). All other reagents were of analytical grade.

EPS extraction and purification The fungal endophyte was cultivated using the method described by Pan et al. (20). Fungal mycelia were separated from the culture broth by vacuum filtration after fermentation. The filtrate was collected and concentrated to 10% of the original volume in a vacuum rotary evaporator at 50–65°C. The concentrated filtrate was successively partitioned three times with equal volumes (v/v) of petroleum ether, ethyl acetate, and *n*-butyl alcohol to remove partial lipids, pigments and so on. Four-volume of ethanol was added, and then a precipitate was allowed to form overnight (12 h) at 4°C. After centrifugation (4000 ×*g*) for 30 min, the precipitate was collected, washed with ethanol, and redissolved in hot water (50°C) and the protocol above was repeated a second time. Finally, the precipitation was collected and lyophilized.

The crude EPS was dissolved distilled water (50 mL) and decolorized by S-8 and D101 macroporous resins following the method of Liu et al. (21) and Yang et al. (22) with some modifications. Dynamic adsorptions were carried out as follows: 50 mL of crude EPS solution was continuously loaded onto an S-8 resin wet-packed glass column (3.0 × 40 cm) at 1.5 mL min^{-1}. Then, the S-8 resin column was eluted with distilled water (25 mL). The eluate was collected, and the same procedure was repeated twice with clean S-8 resin. The D101 resin was used to further decolorize the EPS using the same protocol. The eluted fractions were collected and lyophilized before use.

Protease (trypsinase and papain) in combination with Sevag reagent was used to deproteinize the material (23). The EPS obtained above was dissolved in 50 mM phosphate-buffered saline (PBS, pH 7.4) at a final concentration of 100 mg mL^{-1}. Trypsinase was added to the mixture to give a final concentration of 5 U mL^{-1}, and the solution was maintained at 37°C for 3 h to remove the proteins, and then it was centrifuged at 4000 ×*g* for 10 min. Papain was added to the supernatant at a final concentration of 5 U mL^{-1}, and the mixture was maintained at 55°C for 3 h. Thereafter, the protein residues were removed using Sevag reagent, and the Lowry protein assay (24) was used to determine if the protein was completely removed. Then, protein-free EPS was dialyzed against distilled water for 2 days and freeze dried.

EPS separation The crude EPS (1.0 g) was dissolved in distilled water (2 mL) and was separated on a DEAE cellulose DE-52 column (31.2 × 195 mm) using a linear gradient of deionized water and 0.1 M NaCl as the mobile phases at flow rate of 0.5 mL min^{-1} at room temperature. The eluents (10 mL·$tube^{-1}$) were collected using an automatic collector (BioFrac Fraction collector; Bio-Rad, Hercules, CA, USA). Each fraction was further purified by gel permeation chromatography (Sephadex G-150, 1.5 cm × 50 cm) with NaCl solutions (10 mM) at a flow rate of 0.5 mL min^{-1}. The eluents (5 mL·$tube^{-1}$) were collected. Each fraction was analyzed at 490 nm by the phenol-sulfuric acid colorimetric method. The EPS fractions were concentrated using a rotary evaporator at 50–65°C, dialyzed for one day (to remove the NaCl), and lyophilized to yield powdered samples.

UV spectroscopic analysis The UV spectra of the EPS solutions (1.0 mg mL^{-1}) were recorded with a UV-2450 spectrophotometer (Shimadzu Corporation, Kyoto, Japan) in the 200–400 nm region.

Scanning electron microscopy analysis The EPSs were mounted and modified with a thin layer of gold under reduced pressure. They were then examined using a scanning electron microscopy (SEM) system (JSM-6390A, JOEL, Tokyo, Japan) at an acceleration voltage of 15 kV and at a magnification of 1000×.

Determination of the EPS M_r distribution The EPS M_r distribution was evaluated by high-performance gel-permeation chromatography (HPGPC) (25) on a Waters 1525 HPLC system (Waters, Milford, MA, USA) equipped with a TSK-GEL G5000PWXL column (7.8 mm × 30 cm) and coupled with an evaporative light-scattering detector (ELSD, Alltech, Deerfield, IL, USA). An Alltech 2000ES chromatography station (Zhejiang University, Hangzhou, China) was used. The column was calibrated with deionized water as the mobile phase at a rate of 0.5 mL min^{-1}. The temperature for the detector drift tube was set at 115°C, and the pressurized air flow-rate 3.2 L min^{-1}. The sample injection volume was 10 μL. The sample was then eluted with deionized water as the mobile phase at the same rate. T-series dextran standards (T-5, T-10, T-40, T-70 and T-500) were used to prepare an HPGPC-ELSD calibration curve with the natural logarithm of the M_r plotted as a function of the retention time (*RT*).

Determination of the total polysaccharide content The total polysaccharide contents of the samples were determined by the previously reported phenol-sulfuric acid method using dextran (Mw: 1.26 kDa) as a reference (26) with some modifications. To 60 μL of 5% phenol and 1.5 mL of concentrated sulfuric acid, 100 μL of dextran in a series of concentrations (0.1–1.0 mg mL^{-1}) or sample was added. This mixture was incubated at 25°C for 60 min. The absorbance was measured at 490 nm against a blank using a spectrophotometer. The total polysaccharide content was calculated based on the absorbance value using the following calibration curve: $Y = 0.9678X - 0.0218$, $R^2 = 0.9958$, where Y and X are the absorbance of the tested sample and the ratio of the total polysaccharide, respectively.

Monosaccharide composition analysis The monosaccharide components in A14EPS-1 and A14EPS-2 were determined by PMP precolumn derivatization with high-performance liquid chromatography (PMP-HPLC) of the hydrolysate obtained under strongly acidic conditions as previously described (27,28). The EPS together with an internal standard (fucose) was hydrolyzed with trifluoroacetic acid (TFA) at 90°C for 8 h in a 10-mL sealed ampoule filled with argon gas. After the reaction, the mixture was cooled and transferred to 1.5-mL Eppendorf (EP) tubes and then centrifuged at 12,000 ×*g* for 2 min. After the excess acid in the supernatant was completely removed, the products of the hydrolysis (100 μL) and the stock solution of the standard (each 3 mg) were dissolved in 0.3 M aqueous NaOH (400 μL) and derivatized with 1-phenyl-3-methyl-5-pyrazolone (PMP, 200 μL) at 70°C for 1 h to strengthen the UV absorption. The mixture was cooled to room temperature and neutralized by adding HCl solution. The resulting solution was partitioned twice with chloroform 1:1 (v/v). The aqueous layer was collected and passed through a 0.45 μm membrane for HPLC analysis.

The monosaccharide derivatives were analyzed on an Agilent 1100 series instrument (Agilent, Santa Clara, CA, USA) equipped with a Phenomenex Luna 5 μm C18(2) 100 Å column (250 × 4.6 mm i.d., 5 μm) (Phenomenex, Allerød, Denmark) with 17% acetonitrile/83% PBS (0.1 mM, pH 7.0, v/v) as the eluent at a flow rate of 1 mL min^{-1} at 30°C, and the eluate was monitored at 245 nm. The injection volume was 15 μL.

I_2-KI analysis To a sample solution (0.5 mg mL^{-1}) of the same volume, 2 mL of I_2-KI (containing 0.02% I_2 and 0.2% KI solution) was added, and the solution was mixed. Then, the mixed solution (200 μL) was added to water (800 μL), and changes in color were observed. The absorbance of the mixed solution was measured with a UV–Vis spectrometer in the range of 300–800 nm (29).

Partial acid hydrolysis EPS (80 mg) was hydrolyzed by 0.05 M TFA at 90°C for 2 h in a sealed 10-mL ampoule filled with argon gas. Ethanol was added into the hydrolysate and evaporated to dryness until no acidic vapor remained. The hydrolysate was dissolved in distilled water (5 mL) and added to 45 mL of absolute ethyl alcohol. The precipitate (named A14EPS-1(a)) and the soluble part (named A14EPS-1(b)) were recovered by centrifugation and vacuum dried. A14EPS-1(a) and A14EPS-1(b) were further hydrolyzed by 3 M TFA for 5 h at 90°C. The glycosyl residue contents of A14EPS-1(a) and A14EPS-1(b) were analyzed using TLC (30).

Fourier transform infrared spectroscopy analysis Fourier transform infrared (FT-IR) spectroscopy was performed on a PerkinElmer Spectrum 100 FT-IR spectrophotometer (PerkinElmer Inc., Waltham, MA, USA) to obtain compositional information on the EPS samples. A14EPS-1 and A14EPS-2 were analyzed using the KBr disc method in the frequency range of 4000–450 cm^{-1}.

Nuclear magnetic resonance analysis Samples of A14EPS-1 and A14EPS-2 were dissolved in 0.5 mL D_2O for nuclear magnetic resonance (NMR) analysis. Spectra were recorded on a Bruker Advance spectrometer (Bruker, Switzerland) for ^1H NMR (600 M) and ^{13}C NMR (150 M). The spectra processing and analysis was performed with MestreNova software (Mestrelab Research Inc., Santiago de Compostela, Spain).

Ability of A14EPS-1 and A14EPS-2 to scavenge ABTS radicals The ABTS radical scavenging activity was measured by the improved ABTS method as proposed by Tao et al. (31) with some modifications. Briefly, 180 μL of ABTS solution was added to 30 μL of sample solution (0.1–8.0 mg mL^{-1}). After incubation at 37°C for 5 min in the dark, the absorbance was determined by measuring the UV absorbance at 734 nm against deionized water as a blank using a Multiskan Go microplate reader (MGM, Thermo Scientific, Hampton, NH, USA). The EPS was replaced with water to prepare the control. Ascorbic acid (Vc) was used as the standard antioxidant. The antioxidant capacity was expressed as the percentage decrease in the absorbance at 734 nm, which was calculated using the formula:

$$\text{ABTS radical cation inhibition (\%)} = (1 - A_{sample}/A_{control}) \times 100 \quad (1)$$

where $A_{control}$ is absorbance of the control and A_{sample} is absorbance of a tested sample at the end of the reaction.

Ability of A14EPS-1 and A14EPS-2 to scavenge DPPH radicals The DPPH radical scavenging activity was performed according to the method of Jeong et al. (32) with minor modifications. Briefly, A14EPS-1 and A14EPS-2 were dissolved in distilled water at various final concentrations (0.1–8.0 mg mL^{-1}). The test sample (70 μL) was added to 180 μL of 0.004% DPPH in ethanol (v/v) and incubated at 27°C for 5 min in a microplate well. Then, the absorbance was measured at 517 nm against a deionized water blank using an MGM. The EPS was replaced with water to prepare the control, and Vc was used as the standard antioxidant. The ability to scavenge DPPH radical is expressed as:

$$\text{DPPH radical scavenging ability (\%)} = (1 - A_{sample}/A_{control}) \times 100 \quad (2)$$

where A_{sample} is absorbance of a tested sample at the end of the reaction and $A_{control}$ is absorbance of the DPPH radical solution when the EPS was replaced with water. All of the measurements were performed at least in triplicate.

Reduction power of A14EPS-1 and A14EPS-2 (ferric ion-reducing antioxidant power assay) The total reduction power was measured using the ferric ion-reducing antioxidant power (FRAP) assay. The protocol was executed as described by Pan et al. (33). The FRAP values are expressed on a fresh-weight basis as μmol of ferrous equivalent Fe(II) per L of sample. Vc was used as the standard antioxidant. All of the measurements were performed at least in triplicate.

The antiproliferation activities of A14EPS-1 and A14EPS-2 The *in vitro* antitumor activities of A14EPS-1 and A14EPS-2 were determined by a colorimetry method (34) with some modifications. The human hepatoma cell line HepG2 was cultured in DMEM supplemented with 10% (v/v) FBS with 5% CO_2 at 37°C. Fresh medium was added to the culture broths every 24 h. The cell suspension (0.5-1×10^4 cells mL^{-1}) was then incubated in a 96-well plate (50 μL $well^{-1}$) for 24 h. A14EPS-1 or A14EPS-2 (50 μL) was added to each well at final concentrations of 0.0125, 0.0625, 0.125, 0.25, 0.5 and 1 mg ml^{-1}. Dimethyl sulfoxide was used as a positive control. After incubation for 48 h, the absorbance was measured at 450 nm using a cell counting kit (CCK-8) (35).

$$\text{Growth inhibition ratio} = (OD_0 - OD_s)/OD_0 \times 100\% \quad (3)$$

where OD_0 is the OD at 450 nm of the negative control (water) and OD_s is the OD at 450 nm of the polysaccharide-treated sample. Three wells were set up for each set of conditions, and all samples were tested in triplicate.

RESULTS AND DISCUSSION

Extraction, purification and separation of EPS The contents of pigments and proteins in the crude EPS secreted from strain A14 were very high. S-8 and D101 macroporous resins offer good simultaneous decolorization and deproteinization of the crude EPSs extracted from microorganisms (21,22). Therefore, they were selected to remove the pigments and partial proteins from the crude EPS. The application of proteinase in combination with Sevag reagent can remove most proteins while avoiding the loss of EPS (23). Trypsinase and papain were used to remove the proteins and then Sevag reagent was used to remove the remaining protein including the added proteinases.

After purification using cellulose DE-52 anion exchange chromatography, two independent elution peaks, namely, A14EPS-1 (eluted by water, the major fraction), A14EPS-2 (eluted by 0.1 mol/L NaCl), were obtained (Fig. 1A). Usually, the neutral polysaccharide in the mixture is first eluted by deionized water, and the acidic polysaccharide is then eluted at a higher salt concentration on the cellulose DE-52 anion exchange column (36,37). However, partial neutral polysaccharides can be obtained by eluting with a salt solution because the cellulose DE-52 has both anion exchange and molecular sieve-like properties. The salt solution could exchange the polysaccharide anions with its own anions, allowing the polysaccharide to elute with the water in the solution. Therefore, A14EPS-1 may be a neutral polysaccharide, while A14EPS-2 may be either a neutral or acidic polysaccharide.

Then, A14EPS-1 and A14EPS-2 were further analyzed using a Sepharose G-150 gel filtration column. Single peaks were observed in those chromatograms (Fig. 1B, C), indicating that A14EPS-1 and

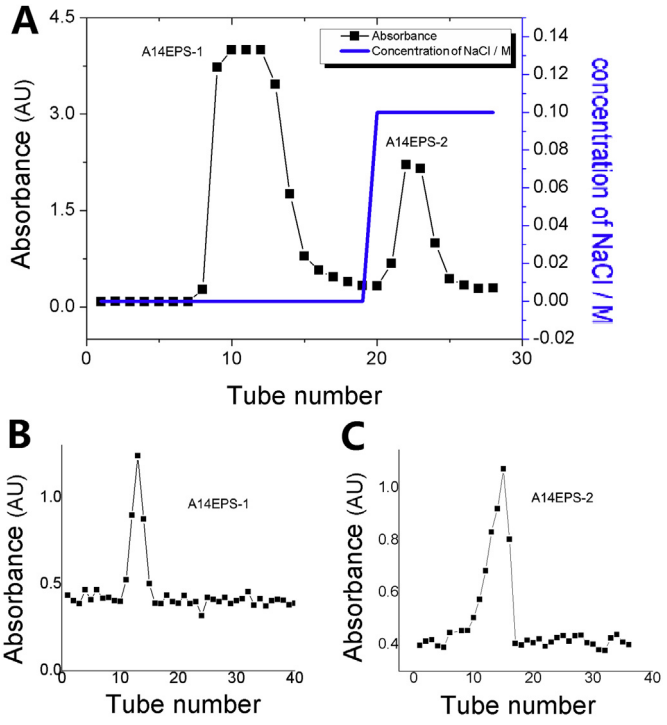

FIG. 1. Elution chromatograms of (A) the crude EPS extracted from the fermentation broth of strain A14 on a DEAE-cellulose column, and the two fractions A14EPS-1 (B) and A14EPS-2 (C) on a Sepharose G-150 gel filtration column.

A14EPS-2 were homogeneous EPS. In addition, for partial EPSs, there is a one-to-one relationship between the fractions and quantities of the EPSs, such as the PRG1 from Russula griseocarnosa sporocarp which was a homogeneous EPS after purification on a DEAE-52 cellulose column (38). In addition, those results indicate that it is not necessary to use a Sephadex column for purification after using a cellulose anion exchange column for EPSs that were homogeneous obtained only by anion exchange chromatography.

UV absorption and SEM analysis The UV spectra of A14EPS-1 and A14EPS-2 are shown in Fig. 2A. Proteins and nucleic acids absorb at 280 nm and 260 nm, respectively (39). No significant absorption from 260 to 280 nm was observed in the UV spectrum of A14EPS-1 and A14EPS-2, indicating that the two EPSs were of high quality and did not contain proteins and nucleic acids. These results indicated that the pigment, protein and nucleic acid impurities were reduced.

SEM analysis of surface morphology is a qualitative tool to characterize fungal EPSs (40). The SEM images of A14EPS-1 and A14EPS-2 are shown in Fig. 2B. The results showed different physical changes were induced by different material. Fig. 2B shows that A14EPS-1 had a rough surface with characteristic linear clavate grain, while A14EPS-2 had a smooth appearance with some cracking. In addition, the SEM image of xylan (small platelets) was quite different from that of the modified xylans at different temperatures with nitrogen (like platelets fused together at their edges) (41). The SEM images show that those two EPSs have distinctly different features on their surfaces, which may reflect their distinctly different structural features.

The EPS M_r distribution analysis Molecular weight is an important structural feature of polysaccharides. The RTs of A14EPS-1 and A14EPS-2 on the HPGFC chromatograms were 17.927 and 20.125 min, respectively. The M_r values of A14EPS-1 and A14EPS-2 were approximately 24 kDa and 5 kDa, respectively, based on linear regression generated from different standard dextrans (ln

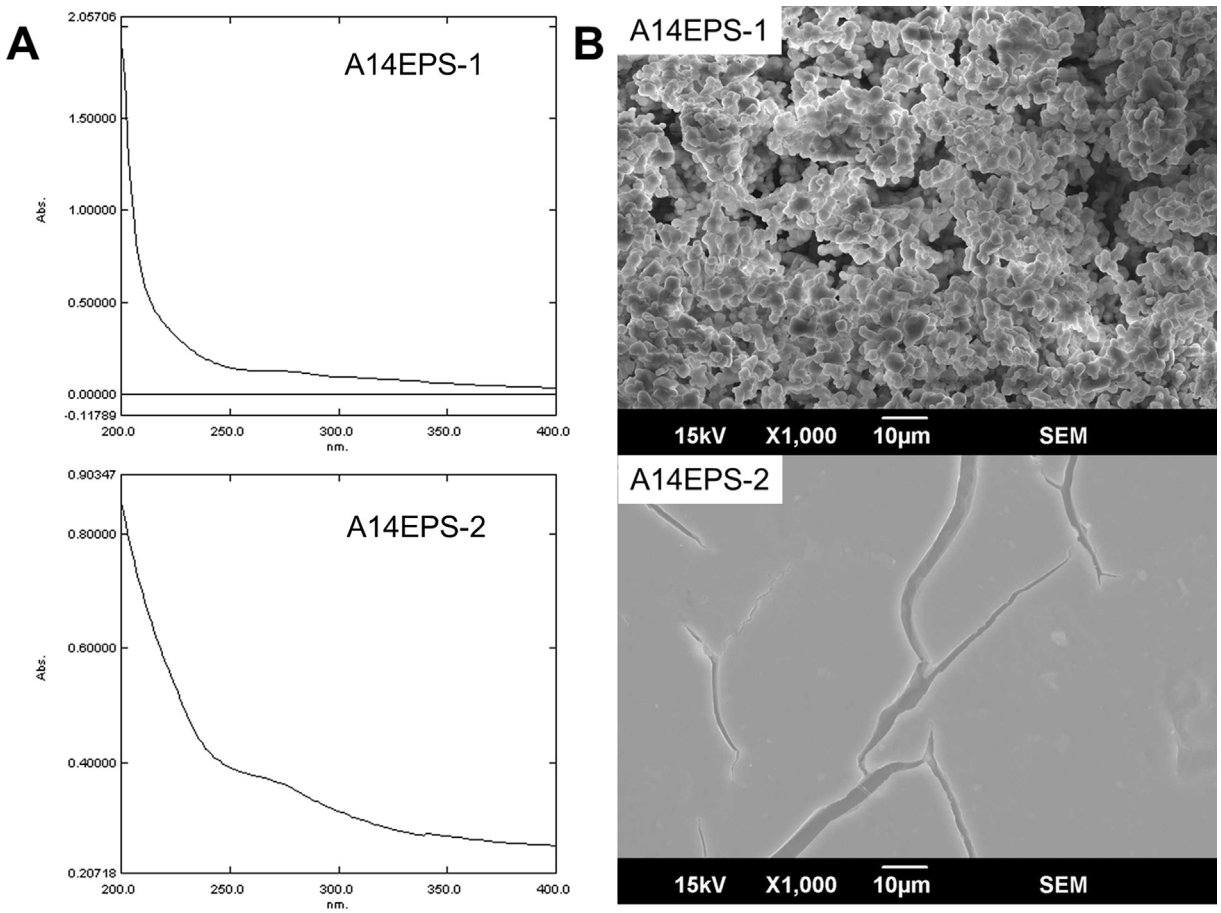

FIG. 2. Characterization of the two EPSs (A14EPS-1 and A14EPS-2) by (A) UV spectroscopy (200–400 nm) and (B) scanning electron microscopy. Bars: 10 μm.

(M_r) = −13.491 ln (RT) + 49.033, R^2 = 0.9793). There was a significant difference between the M_r values of A14EPS-1 and A14EPS-2. The M_r of A14EPS-1 was nearly 4 times that of A14EPS-2. Many reports suggested that the M_r of polysaccharides can significantly affect their biological activities, such as their antioxidant activity. Polysaccharides with low molecular weights may have stronger antioxidant activities since they have more reductive terminal hydroxyl groups to accept and eliminate free radicals (42). For example, the polysaccharide PW3, with molecular weights ranging from 5.3×10^3 to 2.3×10^4 Da, showed better reducing power, metal ion chelating ability, and scavenging abilities against DPPH and ABTS radical than the PS PW1 (1.2×10^5 to 6.3×10^6 Da) and PW2 (3.5×10^4 to 7.4×10^4 Da) (43). Hence, A14EPS-2 may have stronger bioactivity than A14EPS-1.

Total polysaccharide content and monosaccharide analysis The phenol-H_2SO_4 colorimetric assay showed that the weight percentage of total polysaccharide contents of A14EPS-1 and A14EPS-2 were 61.6% and 75.1%, respectively (supplementary Table S1).

The monosaccharide compositions of A14EPS-1 and A14EPS-2 are summarized in Fig. 3 and supplementary Table S1. A14EPS-1 was mainly composed of mannose, rhamnose, glucose, galactose, xylose and arabinose with a molar ratio of 0.31:0.55:10.00:0.34:0.03:0.06, while A14EPS-1 mainly consisted of mannose, rhamnose, glucose, galactose, xylose and arabinose with a molar ratio of 0.16:0.88:10.00:0.39:0.06:0.06. Compositional analysis of the EPSs showed that glucose was the major monosaccharide of the two heteropolysaccharide fractions, while xylose and arabinose were the least abundant monosaccharides. Glucose, which is 88.57% and 86.58% of A14EPS-1 and A14EPS-2, respectively, was found to be one of the most significant factors impacting EPS production, and it is the main monosaccharide in many EPSs from endophytic fungi (8). The results also showed that both A14EPS-1 and A14EPS-2 might be neutral polysaccharides because neither contains galacturonic acid.

The A14EPS-1 fraction was further analyzed using the I_2-KI method since not only was it the major fraction of the EPS, but it also showed a granular appearance like starch tablets in the SEM micrographs (Fig. 2B). I_2 can form a blue complex with starch and serve as an indicator of starch in samples. Supplementary Fig. S1A shows that the I_2-KI-A14EPS-1 reaction was negative, indicating that there was no starch in the A14EPS-1 solution. In addition, I_2 can form special complexes with polysaccharides; complexes displaying an absorption peak at a wavelength of 565 nm indicate that the polysaccharides have fewer branches and shorter side chains (29). Supplementary Fig. S1B shows that there was no obvious absorption peak at 565 nm. The results indicate that A14EPS-1 has more branches and longer side chains. These results were similar to those of PS FWPS1-1 from *F. unibracteata* var. *wabuensis*, which also has branches and longer side chains (44).

Partial acid hydrolysis can be used to analyze the monosaccharide composition of the side chains and backbone of EPSs. I_2-KI assay results indicated that A14EPS-1, the major fraction, has more branches and longer side chains. In addition, the side chain linkages of EPSs are typically more easily hydrolyzed by acid than the backbone (7). Therefore, A14EPS-1 was selected for partial acid hydrolysis. The results are shown in Fig. 4 and indicated that A14EPS-1(a) was composed of rhamnose, arabinose, glucose and

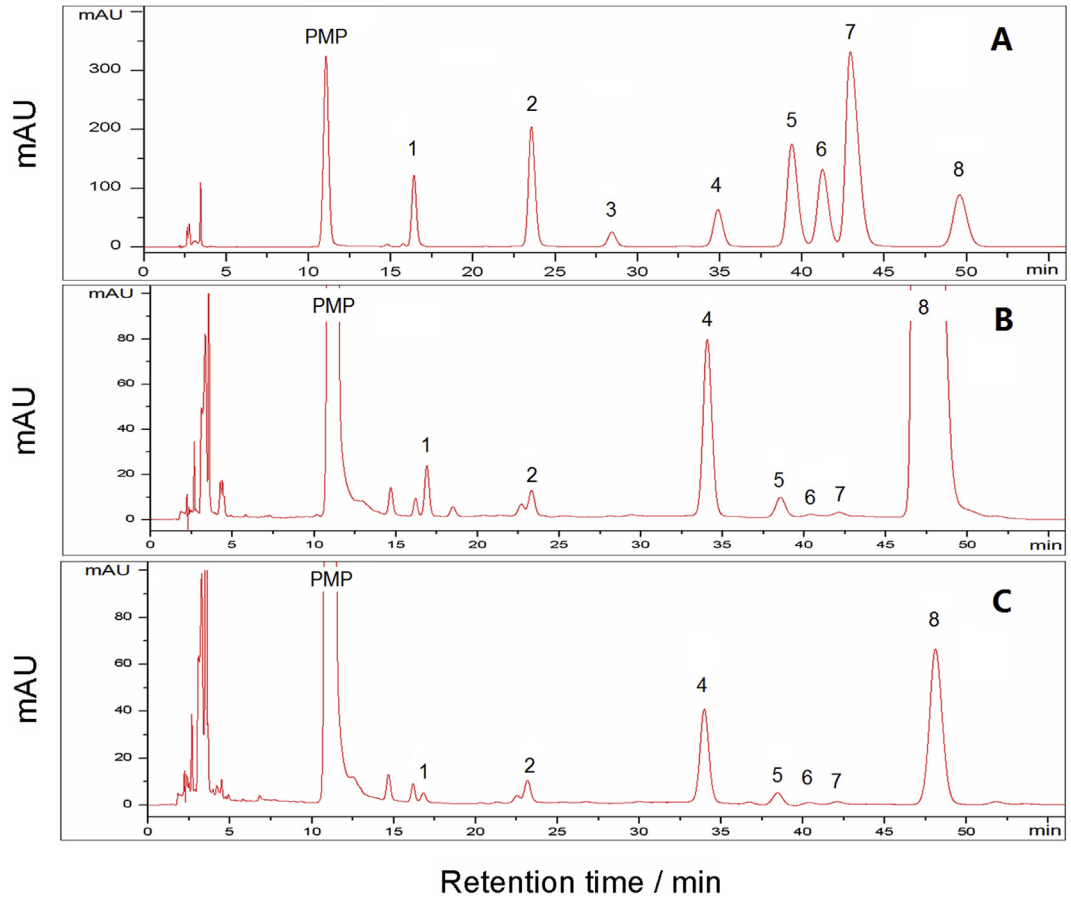

FIG. 3. PMP-HPLC chromatographs of monosaccharide standards (A), A14EPS-1 (B) and A14EPS-2 (C). 1, mannose; 2, rhamnose; 3, galacturonic acid; 4, glucose; 5, galactose; 6, xylose; 7, arabinose; and 8, fucose.

galactose, suggesting that the side chains of A14EPS-1 may be composed of rhamnose, arabinose, glucose and galactose; moreover, A14EPS-1(b) was composed of rhamnose, xylose, arabinose and glucose, suggesting that the backbone of A14EPS-1 may be composed of rhamnose, xylose, arabinose and glucose. Compared with the composition of the original A14EPS-1 EPS, the partially degraded products (A14EPS-1(a) and A14EPS-1(b)) still showed three types of residues (rhamnose, arabinose and glucose). Nearly all the galactose residues are located in the side chains of A14EPS-1, and nearly all the xylose residues are located in the backbone.

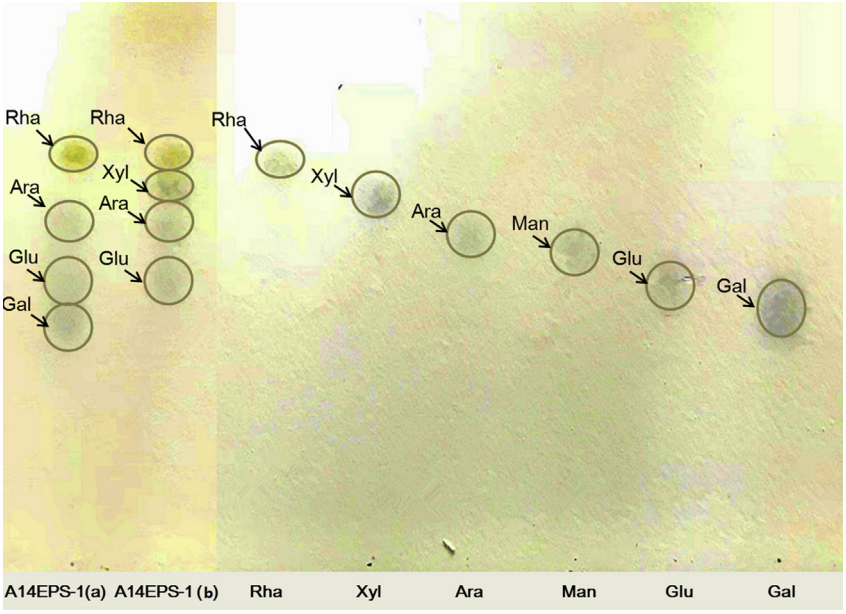

FIG. 4. Thin layer chromatography (TLC) spots showing the monosaccharides constituents from the polysaccharide fractions A14EPS-1(a) and A14EPS-1(b) and the positive monosaccharides.

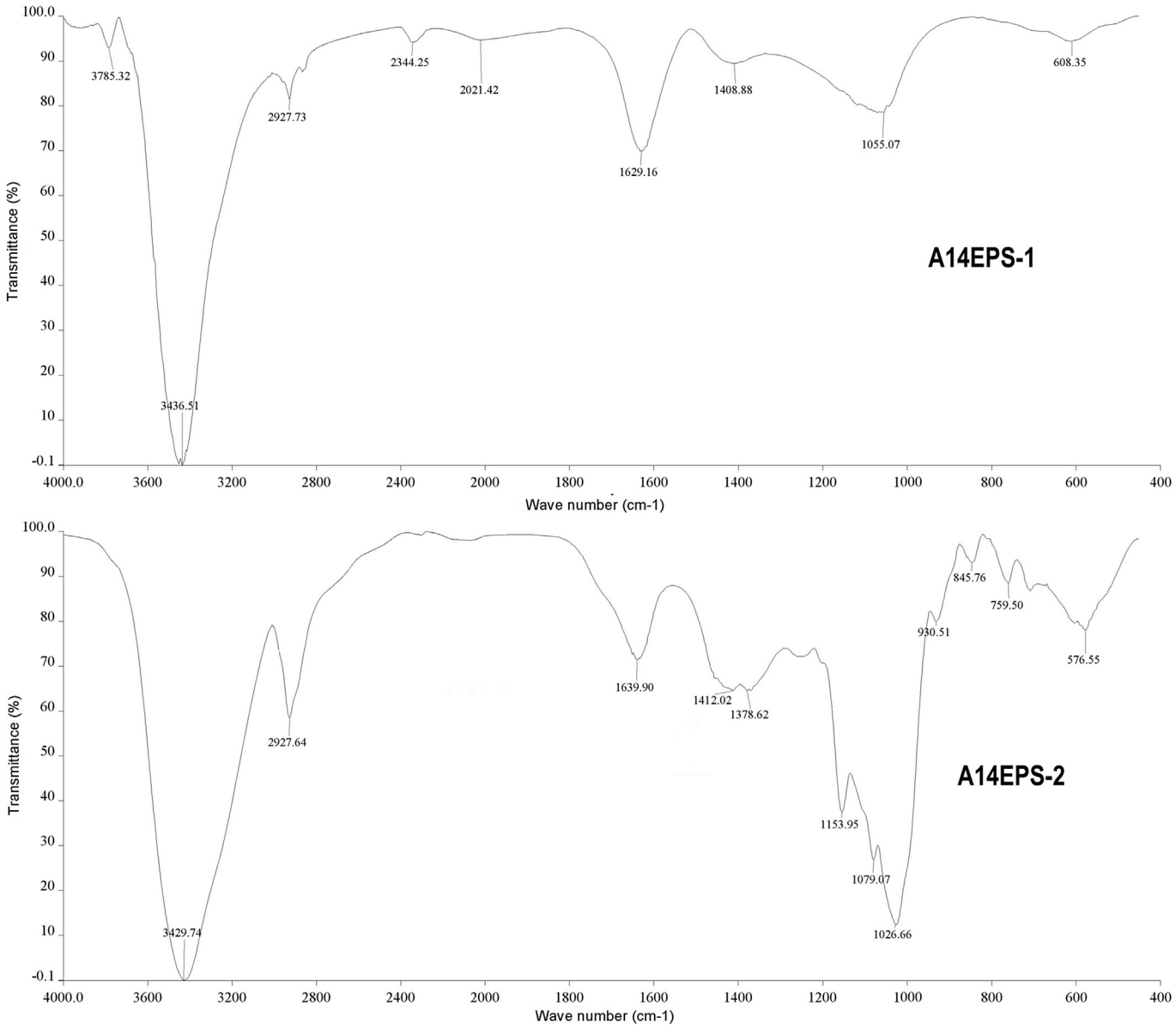

FIG. 5. FT-IR spectrum of A14EPS-1 and A14EPS-2.

FT-IR spectrum FT-IR spectroscopy is a powerful technique for the identification of characteristic organic groups in EPS. The FT-IR spectra of A14EPS-1 and A14EPS-2 are shown in Fig. 5. The broad stretching peaks at 3436.51 cm^{-1} (A14EPS-1) and 3429.74 cm^{-1} (A14EPS-2) were attributed to hydroxyl stretching vibrations. The weak absorption peaks at 2927.73 cm^{-1} (A14EPS-1) and 2927.64 cm^{-1} (A14EPS-2) were characteristic of C—H stretching vibrations of $-CH_2$ moieties (45). In addition, the bands at 1408.88 cm^{-1} (A14EPS-1) and 1412.02 cm^{-1} (A14EPS-2) were assigned to C—H bending vibrations (46). The C—H stretching vibrations and bending vibrations are characteristic absorption peaks of EPSs. The stretching peaks at 1629.16 cm^{-1} (A14EPS-1) and 1639.90 cm^{-1} (A14EPS-2) were due to the bound water (47). This may be the one reason why the weight percentages of total saccharides in A14EPS-1 and A14EPS-2 were not 100%. Moreover, each polysaccharide has a specific band in the 1200-1000 cm^{-1} region. Only one peak (1100—1010 cm^{-1}) in the spectrum of A14EPS-1 or the three stretching peaks at 1153.95 cm^{-1}, 1079.07 cm^{-1}, and 1026.66 cm^{-1} in the spectrum of A14EPS-2 indicated the pyranose form of sugars (46,48,49). In addition, the peaks at 1079.07 cm^{-1} and 1026.66 cm^{-1} in A14EPS-2 were dominated by ring vibrations overlapped with stretching vibrations of (C—OH) side groups and the (C—O—C) glycosidic bond vibration (47,50). The signal at 845.76 cm^{-1} in the spectrum of A14EPS-2 was attributed to the α-glycosidic linkages in the polysaccharide chains. The absorption peaks at 930.51 and 759.50 cm^{-1} in the spectrum of A14EPS-2 suggested the presence of α-D-glucopyranose (α-D-Glcp) (51). From the results described above, it could be concluded that A14EPS-2 was composed primarily of α-pyranose-type sugars. In addition, α-D-glucopyranose might be the main chain of A14EPS-2. However, the type of glycosidic linkages could not be confirmed due to the presence of the indistinct characteristic absorption bands between 800 and 900 cm^{-1} in the spectrum of A14EPS-1. A14EPS-2 had more functional groups than A14EPS-1. This situation is similar to previous reports that the polysaccharide MPS-1 from mulberry leaves contained more distinct functional groups than MPS-2 (48). This result also shows that FT-IR

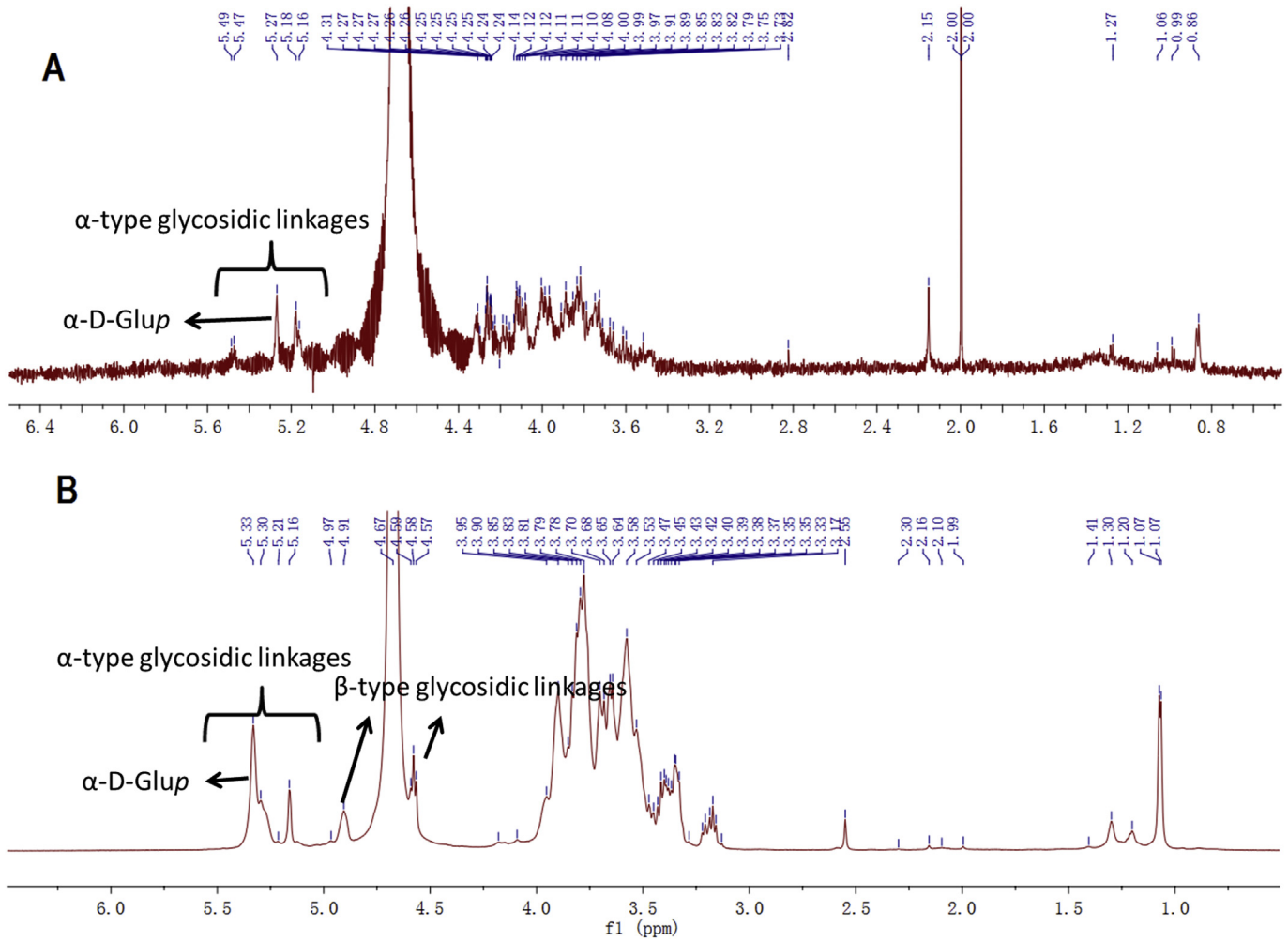

FIG. 6. The ^{1}H NMR (600 MHz, D_2O) spectra of A14EPS-1 (A) and A14EPS-2 (B).

spectroscopy is well-suited for examining the main functional characteristics of EPSs from endophytic fungi.

^{1}H and ^{13}C NMR analysis Signals within the range of 3.0–5.5 ppm (^{1}H NMR) and 60–110 ppm (^{13}C NMR) are characteristic of polysaccharides. The ^{1}H NMR spectra of A14EPS-1 and A14EPS-2 are shown in Fig. 6A and B, respectively. In the ^{1}H NMR spectrum of A14EPS-1, the anomeric resonances at 5.47, 5.27 and 5.18 ppm indicated that this material was mainly composed of three types of pyranose sugars residues and they were primarily in the α-configuration. In addition, the highest intensity signal at 5.27 ppm can be assigned to the anomeric protons of α-D-glucose residue (52). For A14EPS-2, the anomeric proton signals at 5.33, 5.30, 5.21 and 5.16 ppm were characteristic of four α-type glycosidic linkages, and the signals at 4.97, 4.91, 4.59, 4.58 and 4.57 ppm were characteristic of β-type glycosidic linkages, which indicated that A14EPS-2 has both α- and β-configurations. Anomeric protons signals in a relatively high-field region were observed from 5.33 to 5.16 ppm in the ^{1}H NMR spectrum, indicating the glycosidic bonds in A14EPS-2 were mainly α-glycosidic. In addition, the highest intensity signal at 5.33 ppm can attributed to the anomeric protons of the α-D-glucosepyranose residues (53).

The ^{13}C NMR spectrum of A14EPS-2 is illustrated in Fig. 7. The ^{13}C anomeric signals were downfield at ~90 ppm, while the signals of C-2, C-3, C-4 and C-5 appear in the 70–75 ppm region and the signal of C-6 is normally upfield at ~60 ppm (54). Additionally, the anomeric carbon signals at 100.01, 99.80, 99.59, 95.93 and 92.12 ppm were assigned to signals of α-pyranose because the anomeric carbon signal of α-pyranose was downfield and exhibited well-resolved signals characteristic of Glcp, which is similar to what was observed with the polysaccharide from *Cordyceps sinensis* (55). However, the signals of β-pyranose were not measured because of the lower sensitivity of ^{13}C NMR compared to ^{1}H NMR for A14EPS-2. The signals at 16.74 and 17.71 ppm in the ^{13}C NMR were assigned to the methyl groups of rhamnose residues, which agreed with the result of the A14EPS-2 ^{1}H NMR, and the signal at 60.6 ppm was assigned to C-6 of the galactose residue (56). Due to the absence of two-dimensional NMR data, linkage data on the sugar chains is unavailable.

The antioxidant effect The antioxidant effects of A14EPS-1 and A14EPS-2 were evaluated in different *in vitro* models like DPPH and ABTS radical scavenging activity and FRAP activity in a concentration-dependent manner. The results of the DPPH radical scavenging ability compared with that of a positive control, Vc, are shown in Fig. 8A. A14EPS-1 and A14EPS-2 both scavenged DPPH radicals well in a concentration-dependent manner. At relatively low concentrations (0.1–4.0 mg mL^{-1}), A14EPS-1 and A14EPS-2 showed similar scavenging activities, while the latter had a higher scavenging activity (47.22 ± 2.30%) than the former (23.74 ± 4.15%) at a concentration of 8 mg mL^{-1}. The ABTS radical scavenging assay can be separated from the visible-light range with a maximum absorption at 734 nm, and this is usually used

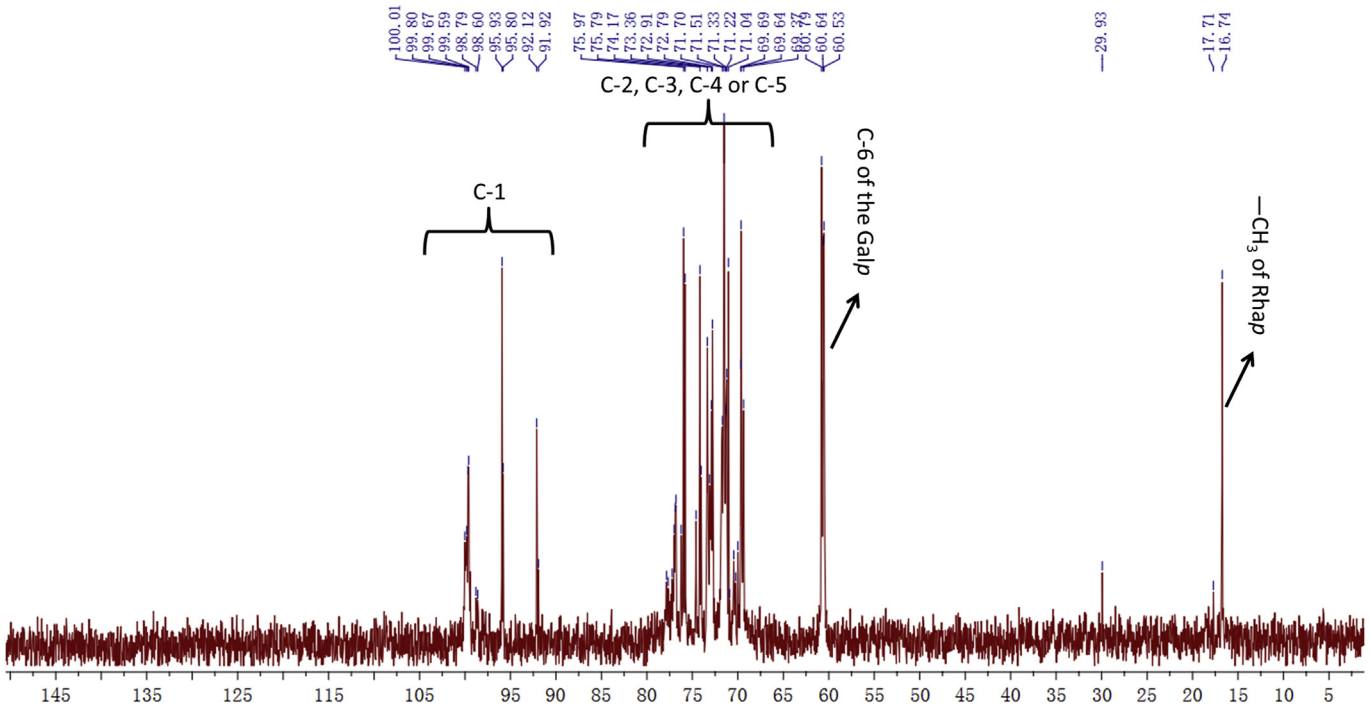

FIG. 7. The ^{13}C NMR (150 MHz, D_2O) spectrum of A14EPS-2.

to evaluate the total antioxidant power of natural compounds (57). As shown in Fig. 8B, A14EPS-1 and A14EPS-2 possessed moderate ABTS radical scavenging capacities in a dose-dependent manner. At a concentration of 8 mg mL^{-1}, their ABTS radical scavenging activities were 29.53 ± 6.30% and 40.67 ± 3.79%, respectively. A14EPS-2 was better able to scavenge ABTS radicals than A14EPS-1, which was similar to the results of the DPPH radical scavenging activities. However, the activities of A14EPS-1 and A14EPS-2 were weaker than that of Vc at the same concentrations for both ABTS and DPPH radicals. The reducing powers of A14EPS-1, A14EPS-2 and Vc are shown in Fig. 8C. Compared with the positive control, A14EPS-1 and A14EPS-2 showed weaker reducing powers, and there were no notable changes when the concentration was increased up to 8 mg mL^{-1}, especially for A14EPS-1. These results

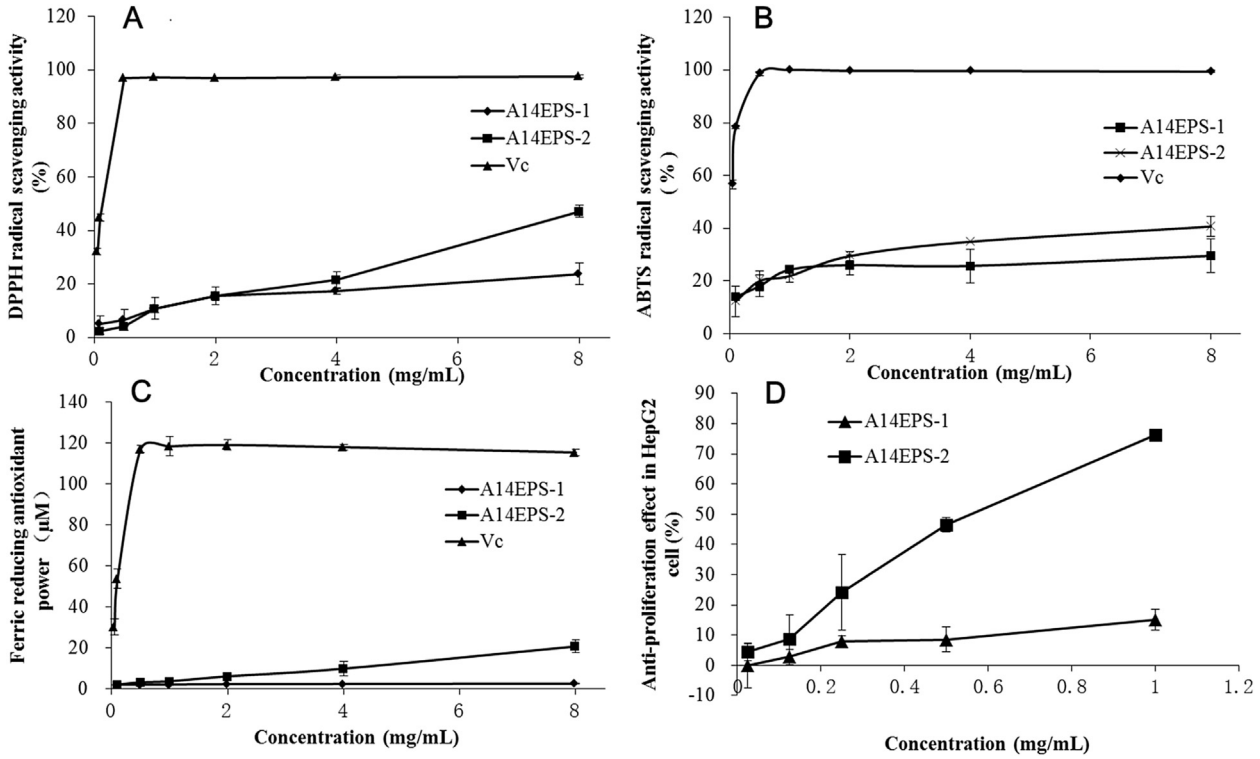

FIG. 8. The antioxidant activities and antiproliferation effects on HepG2 cells of A14EPS-1 and A14EPS-2. (A) DPPH radical scavenging activity; (B) ABTS radical scavenging activity; (C) ferric-reducing power; (D) antiproliferation on HepG2 cells using CCK-8 assays. Data are means ±SD of values obtained from three separate experiments.

indicated A14EPS-1 and A14EPS-2 had moderate antioxidant activities.

Antiproliferation effects on human hepatocellular carcinoma HepG2 cells To investigate the antiproliferation effects of A14EPS-1 and A14EPS-2 on cancer cells, we treated HepG2 cells with the test compounds after incubation in 96-well plates for 24 h. The growth inhibition ratios were calculated based on OD values at 450 nm using a cell counting kit (CCK-8) and the results are shown in Fig. 8D. The antiproliferation effect of A14EPS-1 on HepG2 cell was very poor and showed almost no relationship with the concentration, while A14EPS-2 effectively inhibited HepG2 cell proliferation in a dose-dependent manner with an IC_{50} value of 0.62 mg mL^{-1}. The data suggest that A14EPS-2 can significantly inhibit the growth of human hepatocellular carcinoma HepG2 cells. In addition, these results also showed that polysaccharides from endophytic fungi, such as A14EPS-2 or the EPS from an endophytic fungus *Chaetomium* sp., are unique macromolecules with good antiproliferative activities on cancer cells (58). In addition, compared with the antioxidant results, A14EPS-2 showed stronger bioactivities than A14EPS-1.

In conclusion, in the present investigation we first found that an endophytic fungus, *Fusarium* sp. A14, secreted two water-soluble EPS, namely, A14EPS-1 and A14EPS-2, with M_r values of ~24 kDa and ~5 kDa, respectively. Although they showed similar monosaccharide compositions, noticeable differences were found in their appearance, average molecular weights, structural characteristics, and so on. In addition, both A14EPS-1 and A14EPS-2 had certain antioxidant activity and may be natural antioxidant EPS. In addition, A14EPS-2 also showed a moderate antiproliferation effect on human hepatocellular carcinoma HepG2 cells. The results provide a reference for the large-scale extraction of EPS by endophytic fungus A14 in industrial fermentation and for the development of endogenous fungal resources from *F. unibracteata* Hsiao et KC Hsia.

Supplementary data related to this article can be found at https://doi.org/10.1016/j.jbiosc.2018.07.023.

ACKNOWLEDGMENTS

This work was supported by the Specialized Research Fund for the Doctoral Program of Higher Education, China (grant numbers 20115103110009) and "211" Project Double-Support Plan of Sichuan Agricultural University, China (grant numbers 03570313).

References

1. **Chen, Y., Mao, W., Tao, H., Zhu, W., Qi, X., Chen, Y., Li, H., Zhao, C., Yang, Y., and Hou, Y.:** Structural characterization and antioxidant properties of an exopolysaccharide produced by the mangrove endophytic fungus *Aspergillus* sp. Y16, Bioresour. Technol., **102**, 8179–8184 (2011).
2. **Deng, P., Zhang, G., Zhou, B., Lin, R., Jia, L., Fan, K., Liu, X., Wang, G., Wang, L., and Zhang, J.:** Extraction and *in vitro* antioxidant activity of intracellular polysaccharide by *Pholiota adiposa* SX-02, J. Biosci. Bioeng., **111**, 50–54 (2011).
3. **Yamaguchi, Y. and Koketsu, M.:** Isolation and analysis of polysaccharide showing high hyaluronidase inhibitory activity in *Nostochopsis lobatus* MAC0804NAN, J. Biosci. Bioeng., **121**, 345–348 (2016).
4. **Fialho, A. M., Moreira, L. M., Granja, A. T., Popescu, A. O., Hoffmann, K., and Sá-Correia, I.:** Occurrence, production, and applications of gellan: current state and perspectives, Appl. Microbiol. Biotechnol., **79**, 889–900 (2008).
5. **Freitas, F., Alves, V. D., and Reis, M. A.:** Advances in bacterial exopolysaccharides: from production to biotechnological applications, Trends Biotechnol., **29**, 388–398 (2011).
6. **Chang, S. T. and Wasser, S. P.:** The role of culinary-medicinal mushrooms on human welfare with a pyramid model for human health, Int. J. Med. Mushrooms, **14**, 95–134 (2012).
7. **Li, N., Yan, C., Hua, D., and Zhang, D.:** Isolation, purification, and structural characterization of a novel polysaccharide from *Ganoderma capense*, Int. J. Biol. Macromol., **57**, 285–290 (2013).
8. **Liu, J., Wang, X., Pu, H., Liu, S., Kan, J., and Jin, C.:** Recent advances in endophytic exopolysaccharides: production, structural characterization, physiological role and biological activity, Carbohydr. Polym., **157**, 1113–1124 (2017).
9. **Hao, L., Sheng, Z., Lu, J., Tao, R., and Jia, S.:** Characterization and antioxidant activities of extracellular and intracellular polysaccharides from *Fomitopsis pinicola*, Carbohydr. Polym., **141**, 54–59 (2016).
10. **Ludwig-Müller, J.:** Plants and endophytes: equal partners in secondary metabolite production? Biotechnol. Lett., **37**, 1325–1334 (2015).
11. **Ganley, R. J., Brunsfeld, S. J., and Newcombe, G.:** A community of unknown, endophytic fungi in western white pine, Proc. Natl. Acad. Sci. USA, **101**, 10107–10112 (2004).
12. **Li, P., Lu, S., Shan, T., Mou, Y., Li, Y., Sun, W., and Zhou, L.:** Extraction optimization of water-extracted mycelial polysaccharide from endophytic fungus *Fusarium oxysporum* Dzf17 by response surface methodology, Int. J. Mol. Sci., **13**, 5441–5453 (2012).
13. **Orlandelli, R. C., Vasconcelos, A. F. D., Azevedo, J. L., da Silva, M.d. L. C., and Pamphile, J. A.:** Screening of endophytic sources of exopolysaccharides: preliminary characterization of crude exopolysaccharide produced by submerged culture of *Diaporthe* sp. JF766998 under different cultivation time, Biochim. Open, **2**, 33–40 (2016).
14. **Hiruma, K., Gerlach, N., Sacristán, S., Nakano, R. T., Hacquard, S., Kracher, B., Neumann, U., Ramírez, D., Bucher, M., and O'Connell, R. J.:** Root endophyte *Colletotrichum tofieldiae* confers plant fitness benefits that are phosphate status dependent, Cell, **165**, 464–474 (2016).
15. **Mahapatra, S. and Banerjee, D.:** Optimization of a bioactive exopolysaccharide production from endophytic *Fusarium solani* SD5, Carbohydr. Polym., **97**, 627–634 (2013).
16. **Mahapatra, S. and Banerjee, D.:** Evaluation of *in vitro* antioxidant potency of exopolysaccharide from endophytic *Fusarium solani* SD5, Int. J. Biol. Macromol., **53**, 62–66 (2013).
17. **Li, Y., Guo, S., and Zhu, H.:** Statistical optimization of culture medium for production of exopolysaccharide from endophytic fungus *Bionectria ochroleuca* and its antitumor effect *in vitro*, EXCLI J, **15**, 211–220 (2016).
18. **Aly, A. H., Debbab, A., Kjer, J., and Proksch, P.:** Fungal endophytes from higher plants: a prolific source of phytochemicals and other bioactive natural products, Fungal Divers., **41**, 1–16 (2010).
19. **Chandra, S.:** Endophytic fungi: novel sources of anticancer lead molecules, Appl. Microbiol. Biotechnol., **95**, 47–59 (2012).
20. **Pan, F., Su, X., Hu, B., Yang, N., Chen, Q., and Wu, W.:** *Fusarium redolens* 6WBY3, an endophytic fungus isolated from *Fritillaria unibracteata* var. *wabuensis*, produces peimisine and imperialine-3β-D-glucoside, Fitoterapia, **103**, 213–221 (2015).
21. **Liu, J., Luo, J., Sun, Y., Ye, H., Lu, Z., and Zeng, X.:** A simple method for the simultaneous decoloration and deproteinization of crude levan extract from *Paenibacillus polymyxa* EJS-3 by macroporous resin, Bioresour. Technol., **101**, 6077–6083 (2010).
22. **Yang, R., Meng, D., Song, Y., Li, J., Zhang, Y., Hu, X., Ni, Y., and Li, Q.:** Simultaneous decoloration and deproteinization of crude polysaccharide from pumpkin residues by cross-linked polystyrene macroporous resin, J. Agric. Food Chem., **60**, 8450–8456 (2012).
23. **Zha, X. Q., Xiao, J. J., Zhang, H. N., Wang, J. H., Pan, L. H., Yang, X. F., and Luo, J. P.:** Polysaccharides in *Laminaria japonica* (LP): extraction, physicochemical properties and their hypolipidemic activities in diet-induced mouse model of atherosclerosis, Food Chem., **134**, 244–252 (2012).
24. **Lowry, O. H., Rosebrough, N. J., Farr, A. L., and Randall, R. J.:** Protein measurement with the Folin phenol reagent, J. Biol. Chem., **193**, 265–275 (1951).
25. **Liu, L., Lu, Y., Li, X., Zhou, L., Yang, D., Wang, L., and Chen, Y.:** A novel process for isolation and purification of the bioactive polysaccharide TLH-3' from *Tricholoma lobayense*, Process Biochem., **50**, 1146–1151 (2015).
26. **DuBois, M., Gilles, K. A., Hamilton, J. K., Rebers, P. A., and Smith, F.:** Colorimetric method for determination of sugars and related substances, Anal. Chem., **28**, 350–356 (1956).
27. **Lv, Y., Yang, X., Zhao, Y., Ruan, Y., Yang, Y., and Wang, Z.:** Separation and quantification of component monosaccharides of the tea polysaccharides from *Gynostemma pentaphyllum* by HPLC with indirect UV detection, Food Chem., **112**, 742–746 (2009).
28. **Chen, R., Liu, Z., Zhao, J., Chen, R., Meng, F., Zhang, M., and Ge, W.:** Antioxidant and immunobiological activity of water-soluble polysaccharide fractions purified from *Acanthopanax senticosu*, Food Chem., **127**, 434–440 (2011).
29. **Shi, C. S., Sang, Y. X., Sun, G. Q., Li, T. Y., Gong, Z. S., and Wang, X. H.:** Characterization and bioactivities of a novel polysaccharide obtained from *Gracilariopsis lemaneiformis*, An. Acad. Bras. Ciênc., **89**, 175–189 (2017).
30. **Biringanine, G., Ouedraogo, M., Vray, B., Samuelsen, A. B., and Duez, P.:** Partial chemical characterization of immunomodulatory polysaccharides from *Plantago palmata* Hook. fs leaves, Int. J. Carbohyd. Chem., **2012**, 1–7 (2012).
31. **Tao, Y., Wang, P., Wang, Y., Kadam, S. U., Han, Y., Wang, J., and Zhou, J.:** Power ultrasound as a pretreatment to convective drying of mulberry (*Morus alba* L.) leaves: impact on drying kinetics and selected quality properties, Ultrason. Sonochem., **31**, 310–318 (2016).
32. **Jeong, J. B., Park, J. H., Lee, H. K., Ju, S. Y., Hong, S. C., Lee, J. R., Chung, G. Y., Lim, J. H., and Jeong, H. J.:** Protective effect of the extracts from *Cnidium officinale* against oxidative damage induced by hydrogen peroxide via antioxidant effect, Food Chem. Toxicol., **47**, 525–529 (2009).

33. **Pan, F., Su, T. J., Cai, S. M., and Wu, W.:** Fungal endophyte-derived *Fritillaria unibracteata* var. *wabuensis*: diversity, antioxidant capacities *in vitro* and relations to phenolic, flavonoid or saponin compounds, Sci. Rep., **7**, 42008 (2017).
34. **Chen, Z., Zhang, C., Gao, F., Fu, Q., Fu, C., He, Y., and Zhang, J.:** A systematic review on the rhizome of *Ligusticum chuanxiong* Hort. (Chuanxiong), Food Chem. Toxicol., **119**, 309–325 (2018).
35. **Fan, S., Zhang, J., Nie, W., Zhou, W., Jin, L., Chen, X., and Lu, J.:** Antitumor effects of polysaccharide from *Sargassum fusiforme* against human hepatocellular carcinoma HepG2 cells, Food Chem. Toxicol., **102**, 53–62 (2017).
36. **Chang, S., Hsu, B., and Chen, B.:** Structural characterization of polysaccharides from *Zizyphus jujuba* and evaluation of antioxidant activity, Int. J. Biol. Macromol., **47**, 445–453 (2010).
37. **Guan, J. and Li, S. P.:** Quality control of polysaccharides from medicinal plants and fungi, pp. 31–65, in: Ching, F. M. (Ed.), Chinese herbal drug research trends. Nova Science Publishers Inc., New York (2007).
38. **Liu, Y., Zhang, J., and Meng, Z.:** Purification, characterization and anti-tumor activities of polysaccharides extracted from wild *Russula griseocarnosa*, Int. J. Biol. Macromol., **109**, 1054–1060 (2018).
39. **Anders, C., Niewoehner, O., and Jinek, M.:** *In vitro* reconstitution and crystallization of Cas9 endonuclease bound to a guide RNA and a DNA target, Methods Enzymol., **558**, 515–537 (2015).
40. **Cardozo, F., Camelini, C., Cordeiro, M., Mascarello, A., Malagoli, B., Larsen, I., Rossi, M., Nunes, R., Braga, F., and Brandt, C.:** Characterization and cytotoxic activity of sulfated derivatives of polysaccharides from *Agaricus brasiliensis*, Int. J. Biol. Macromol., **57**, 265–272 (2013).
41. **Ünlü, C. H., Kutlu, M., and Atıcı, O. G.:** Mannich reaction of polysaccharides: xylan functionalization in aqueous basic medium, Carbohydr. Polym., **127**, 19–27 (2015).
42. **Wang, J., Hu, S., Nie, S., Yu, Q., and Xie, M.:** Reviews on mechanisms of *in vitro* antioxidant activity of polysaccharides, Oxid. Med. Cell. Longev., **2016**, 5692852 (2016).
43. **Zha, X. Q., Wang, J. H., Yang, X. F., Liang, H., Zhao, L. L., Bao, S. H., Luo, J. P., Xu, Y. Y., and Zhou, B. B.:** Antioxidant properties of polysaccharide fractions with different molecular mass extracted with hot-water from rice bran, Carbohydr. Polym., **78**, 570–575 (2009).
44. **Pan, F., Su, T. J., Liu, Y., Hou, K., Chen, C., and Wu, W.:** Extraction, purification and antioxidation of a polysaccharide from *Fritillaria unibracteata* var. *wabuensis*, Int. J. Biol. Macromol., **112**, 1073–1083 (2018).
45. **Zheng, Y., Zhang, S., Wang, Q., Lu, X., Lin, L., Tian, Y., Xiao, J., and Zheng, B.:** Characterization and hypoglycemic activity of a β-pyran polysaccharides from bamboo shoot (*Leleba oldhami* Nakal) shells, Carbohydr. Polym., **144**, 438–446 (2016).
46. **Liu, X. C., Zhu, Z. Y., Tang, Y. L., Wang, M. F., Wang, Z., Liu, A. J., and Zhang, Y. M.:** Structural properties of polysaccharides from cultivated fruit bodies and mycelium of *Cordyceps militaris*, Carbohydr. Polym., **142**, 63–72 (2016).
47. **Luo, A., He, X., Zhou, S., Fan, Y., Luo, A., and Chun, Z.:** Purification, composition analysis and antioxidant activity of the polysaccharides from *Dendrobium nobile* Lindl, Carbohydr. Polym., **79**, 1014–1019 (2010).
48. **Ying, Z., Han, X., and Li, J.:** Ultrasound-assisted extraction of polysaccharides from mulberry leaves, Food Chem., **127**, 1273–1279 (2011).
49. **Cai, W., Xie, L., Chen, Y., and Zhang, H.:** Purification, characterization and anticoagulant activity of the polysaccharides from green tea, Carbohydr. Polym., **92**, 1086–1090 (2013).
50. **Guo, S., Mao, W., Li, Y., Gu, Q., Chen, Y., Zhao, C., Li, N., Wang, C., Guo, T., and Liu, X.:** Preparation, structural characterization and antioxidant activity of an extracellular polysaccharide produced by the fungus *Oidiodendron truncatum* GW, Process Biochem., **48**, 539–544 (2013).
51. **Wu, F., Yan, H., Ma, X., Jia, J., Zhang, G., Guo, X., and Gui, Z.:** Comparison of the structural characterization and biological activity of acidic polysaccharides from *Cordyceps militaris* cultured with different media, World J. Microbiol. Biotechnol., **28**, 2029–2038 (2012).
52. **Meng, F. Y., Ning, Y. L., Qi, J., He, Z., Jie, J., Lin, J. J., Huang, Y. J., Li, F. S., and Li, X. H.:** Structure and antitumor and immunomodulatory activities of a water-soluble polysaccharide from *Dimocarpus longan* pulp, Int. J. Mol. Sci., **15**, 5140–5162 (2014).
53. **Cao, W., Li, X. Q., Liu, L., Wang, M., Fan, H. T., Li, C., Lv, Z., Wang, X., and Mei, Q.:** Structural analysis of water-soluble glucans from the root of *Angelica sinensis* (Oliv.) Diels, Carbohydr. Res., **341**, 1870–1877 (2006).
54. **Maina, N. H., Tenkanen, M., Maaheimo, H., Juvonen, R., and Virkki, L.:** NMR spectroscopic analysis of exopolysaccharides produced by *Leuconostoc citreum* and *Weissella confusa*, Carbohydr. Res., **343**, 1446–1455 (2008).
55. **Nie, S. P., Cui, S. W., Phillips, A. O., Xie, M. Y., Phillips, G. O., Al-Assaf, S., and Zhang, X. L.:** Elucidation of the structure of a bioactive hydrophilic polysaccharide from *Cordyceps sinensis* by methylation analysis and NMR spectroscopy, Carbohydr. Polym., **84**, 894–899 (2011).
56. **Chai, Y. and Zhao, M.:** Purification, characterization and anti-proliferation activities of polysaccharides extracted from *Viscum coloratum* (Kom.) Nakai, Carbohydr. Polym., **149**, 121–130 (2016).
57. **Nithiyanantham, S., Siddhuraju, P., and Francis, G.:** A promising approach to enhance the total phenolic content and antioxidant activity of raw and processed *Jatropha curcas* L. kernel meal extracts, Ind. Crop. Prod., **43**, 261–269 (2013).
58. **Zhang, H., Wang, X., Li, R., Sun, X., Sun, S., Li, Q., and Xu, C.:** Preparation and bioactivity of exopolysaccharide from an endophytic fungus *Chaetomium* sp. of the medicinal plant gynostemma pentaphylla, Pharmacogn. Mag., **13**, 477–482 (2017).